Phase evolution during crystallization of nanocomposite alloys with Co:Fe ratios in the two-phase region of the binary Fe–Co phase diagram

P. R. Ohodnicki,[a] S. Y. Park, H. K. McWilliams, K. Ramos, D. E. Laughlin, and M. E. McHenry
Materials Science and Engineering Department, Carnegie Mellon University, Pittsburgh, Pennsylvania, 15213

(Presented on 11 January 2007; received 29 October 2006; accepted 12 December 2006; published online 2 May 2007)

A series of alloys was prepared to investigate the crystallization of Co-rich HiTPerm-type alloys $[(Co_{1-x}Fe_x)_{88}Zr_7B_4Cu_1]$ with Fe:Co ratios within or near the two-phase (bcc+fcc) region of the binary phase diagram. The goal of this work is to better understand the phase evolution and crystallization of alloys in which the Fe–Co binary phase diagram predicts more than one transition metal rich primary crystalline phase to be present in equilibrium at the primary crystallization temperature. X-ray diffraction, transmission electron microscopy, and high-temperature vibrating-sample magnetometry have been performed to identify the first phase to crystallize and to follow the evolution of phases during crystallization. The bcc phase appears to be the primary crystalline phase that forms first after annealing at 450 °C for 1 h, in agreement with previous work on Co-rich nanocomposite alloys. We observe that as the Co concentration is increased, the fcc crystalline phase forms at lower annealing temperatures and its volume fraction increases for a given annealing temperature. © *2007 American Institute of Physics*. [DOI: 10.1063/1.2711283]

INTRODUCTION

Nanocrystalline and amorphous Fe- and Co-based nanocomposite alloys are of interest for a variety of soft magnetic applications.[1] The most commonly studied alloys consist of Fe-rich variants of the well-known Finemet,[2] Nanoperm,[3] and HiTPerm (Ref. 4) compositions, which exhibit a two-phase mixture of nanocrystalline bcc or bcc-derivative primary crystalline phase surrounded by an amorphous matrix enriched in glass formers. Increasingly, Co-rich alloys based on the prototype compositions are being investigated for potential applications in high-frequency inductive components. The increased interest in this composition range is due to the low losses and large field-induced anisotropies obtainable.[5,10]

In previous studies, it has been observed that the bcc or bcc-derivative phase is the first primary crystalline phase to form in many Co-rich (Fe, Co) based nanocomposite alloys when the Co:Fe atomic ratio corresponds to the equilibrium two-phase (fcc+bcc) region of the Fe–Co binary phase diagram. The bcc phase has been observed to form first even when the composition corresponds to the single-phase fcc region.[5,6] For Co-rich compositions studied in Ref. 5, the Co:Fe ratios which exhibited the largest field-induced anisotropy for both (CoFe)SiZrB(Cu) and (CoFe)SiNbB(Cu) alloys were well within the two-phase region of the bulk phase diagram despite the observation of only a single primary crystalline bcc-based phase in the optimized alloys. The current work aims to identify the crystalline phases present at various stages of crystallization for the composition and temperature ranges in which more than one primary crystalline transition metal rich phase is a possible candidate based on predictions using the equilibrium Fe–Co binary phase diagram. An understanding of the evolution of the phases during the crystallization process in these alloys will provide insight into the mechanisms governing the solid-state transformations.

EXPERIMENTAL RESULTS

A series of $(Co_{1-x}Fe_x)_{88}Zr_7B_4Cu_1$ (for $x=0.4$, 0.3, 0.25, 0.2, 0.15, 0.1, and 0.04) amorphous alloys were synthesized by single-roller-wheel melt spinning. The alloys were arc melted using high purity (>99.9% by mole fraction) elemental Fe, Co, Zr, and Cu. B was added using an Fe–B compound provided by Spang Magnetics, which also included trace amounts of Si, C, and Al. The wheel side of the as-cast ribbons were confirmed to be amorphous through x-ray diffraction (XRD) and the air side of the ribbons exhibited significant surface crystallization.

High-temperature vibrating-sample magnetometry was used to identify characteristic phase transformation temperatures on heating the initially amorphous alloys from room temperature to 1000 °C. The crystalline surface layer was polished off before measurements to ensure that the magnetic signal was due only to the initially amorphous phase. An average heating rate of ~4 °C/min in the temperature range of interest was employed. In Fig. 1, the magnetization versus temperature, $M(T)$, plots obtained are illustrated. Two selected $M(T)$ curves are highlighted in Fig. 1(b), which illustrate the procedure for extracting characteristic temperature. Figure 1(b) also illustrates the qualitative difference between $M(T)$ data obtained for alloys with $x > \sim 0.20$ as compared to Co-rich alloys with $x < \sim 0.20$. In the latter case, the Curie temperature, $T_{\mathrm{Curie}\,\gamma}$, of the γ phase lies above the temperature at which all of the bcc has transformed to fcc, and the Curie behavior of the fcc phase is observed as a result. In the former case, the $\alpha(\mathrm{bcc}) \rightarrow \gamma(\mathrm{fcc})$ transformation is marked by a sharp drop in the magnetization as the ferromagnetic bcc phase transforms to paramagnetic fcc phase.

[a]Author to whom correspondence should be addressed; electronic mail: pohodnic@andrew.cmu.edu

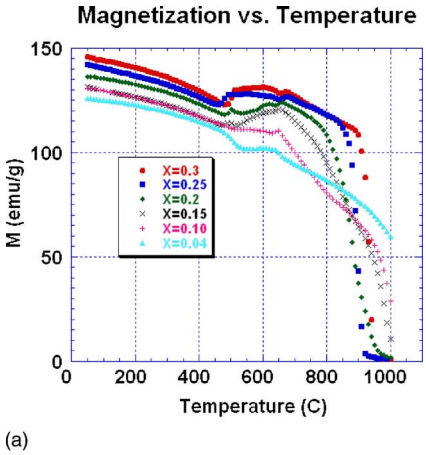

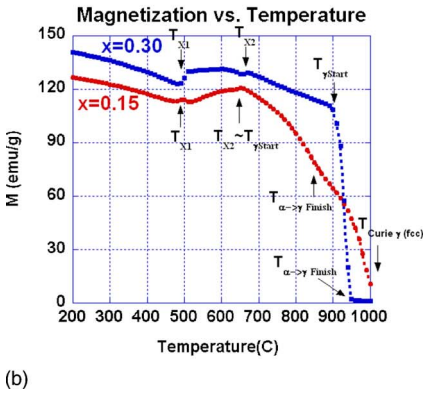

FIG. 1. (Color online) (a) M vs T curves measured for initially amorphous alloys with a heating rate of roughly 4 °C/min on average. (b) Two M vs T curves illustrating the qualitative difference for Co-rich alloys and alloys near equiatomic Co:Fe ratio.

For all alloys, the solid-state phase transformations occurring upon heating consist of primary crystallization of a transition metal rich nanocrystalline phase or phases ($T \sim 450$ °C) followed by secondary crystallization of the remaining amorphous phase ($T \sim 600$ °C). Comparison with XRD results on the wheel side of the ribbons (Fig. 2) after annealing for 1 h at $T=450$ °C shows that only bcc phase is present after this thermal treatment for all but the $x=0.04$ composition, where a minority fraction of fcc phase is also observed. XRD results after annealing at 600 °C show that $(Co,Fe)_2Zr$ and $(Co,Fe)_{23}Zr_6$ appear just after secondary crystallization in all alloys investigated here. In the case of the $x=0.04$ composition, additional peaks present in the XRD patterns could be indexed to the hcp phase after annealing at temperatures above and slightly below that required for the onset of secondary crystallization.

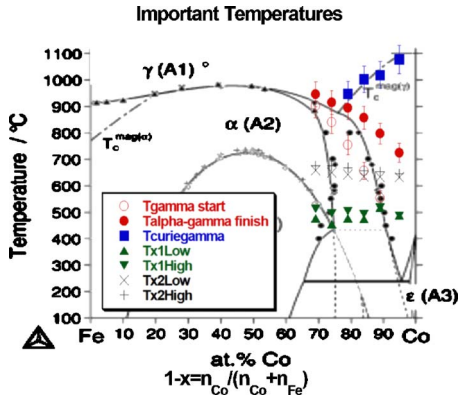

FIG. 3. (Color online) Characteristic temperatures extracted from Fig. 1 compared with the equilibrium binary Fe–Co phase diagram from Ref. 7.

For the Fe-rich nanocomposite alloys, the first primary crystalline phase observed is typically a bcc or bcc-derivative phase and the $\alpha(\text{bcc}) \rightarrow \gamma(\text{fcc})$ transformation is seen as a marked drop in the magnetization over a small temperature range upon formation of the paramagnetic γ phase. In the case of the Co-rich alloys studied here, the bcc phase is still the predominant first phase to form at low temperatures; however, the $\alpha \rightarrow \gamma$ transformation occurs gradually over a wide temperature range. Therefore, formation of the γ phase is indicated by two characteristic temperatures which are referred to in this work as $T_{\gamma,\text{start}}$ and $T_{\alpha \rightarrow \gamma,\text{finish}}$, corresponding to the first temperature at which the γ phase forms in significant amounts and the highest temperature at which bcc phase is present, respectively. It is not yet clear if the first γ phase to form nucleates directly from the amorphous matrix or if it transforms from the bcc nanocrystalline grains.

Because of the finite heating rate, the temperatures extracted from the vibrating-sample magnetometry (VSM) data are characteristic kinetic temperatures and not equilibrium temperatures. Nevertheless, it is useful to compare the extracted temperatures directly with the equilibrium binary Fe–Co phase diagram, taken from, Ref. 7 in Fig. 3. Figure 3 shows that both $T_{\gamma,\text{start}}$ and $T_{\alpha \rightarrow \gamma,\text{finish}}$ decrease with increasing Co content, indicating that fcc phase forms at lower temperatures and that the relative amount of fcc phase is greater at a given temperature as seen in the XRD patterns of Fig. 2. It is evident that the bcc phase tends to crystallize from the amorphous phase in Co-rich HiTPerm alloys more readily

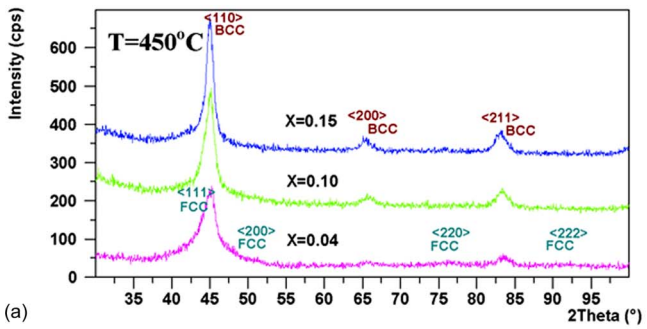

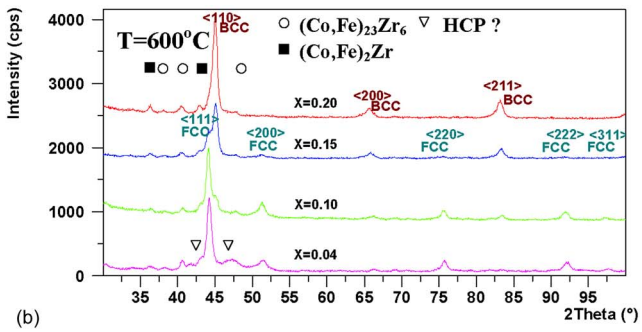

FIG. 2. (Color online) XRD patterns after annealing the initially amorphous ribbons at $T=450$ °C for 1 h, resulting in only primary crystallization, and $T=600$ °C for 1 h, resulting in secondary crystallization.

than one would expect based on the equilibrium binary Fe–Co phase diagram for alloys with the same Co:Fe ratio. These observations are consistent with the experimental results in both Refs. 5 and 6, in which the bcc phase was the first crystalline phase observed to form in Co-rich amorphous/nanocrystalline composites at temperatures far below the secondary crystallization temperature. The present results indicate that the transition from nucleation of a bcc crystalline phase to nucleation of a fcc crystalline phase must occur at Co:Fe ratios that are significantly larger than predicted from the binary phase diagram. The underlying mechanism responsible for this observation is a subject of current investigations.

In addition to the preferential nucleation of bcc phase in the Co-rich alloys, it is also shown that the α phase persists at much higher temperatures than would be expected for a simple binary alloy of the same Co:Fe ratio in equilibrium even after the onset of formation of the γ phase. Although a sharp increase in the relative amount of fcc phase is observed for many alloys at the secondary crystallization temperature (compare the XRD patterns for 450 and 600 °C, 1 h annealing treatments in Fig. 3), bcc phase still persists above the secondary crystallization temperature for the $x=0.1$ alloy, where the kinetics of diffusion are enhanced. Note that no bcc phase would be present at equilibrium in a bulk binary alloy with the same Co:Fe ratio. It is possible that this observation is a primarily kinetic effect.

Since the estimated Curie temperatures of the fcc phase ($T_{\mathrm{Curie}\gamma}$) lie above the maximum temperature at which magnetization measurements can be carried out using the current experimental setup ($T_{\max}=1000$ °C) for many of the alloys, the Curie temperatures were estimated in all cases by squaring the reduced magnetization and extrapolating to $m=M/Ms=0$. We note the good agreement of the experimentally estimated values of $T_{\mathrm{Curie}\gamma}$ with the values predicted from the Fe–Co binary phase diagram as a function of Fe:Co ratio in the initially amorphous alloy as shown in Fig. 3. Although the Curie temperature estimates have significant uncertainty due to the extrapolation technique, it is reasonable to conclude that the Co:Fe ratio in the fcc crystalline phase at these high temperatures ($T\sim 900-1100$ °C) is likely similar to that of the initial amorphous alloy.

DISCUSSION

In this work, we definitively show that the bcc phase preferentially forms first from the amorphous phase for Co-rich HiTPerm alloys, with Co:Fe ratios corresponding to the two-phase region of the binary Fe–Co equilibrium phase diagram. In the case where the Co:Fe ratios of the amorphous and the first bcc crystalline phase to form are identical, one might expect that the T_0 construction first discussed by Massalski[8] may provide some guidance as to the first phase that would be expected to nucleate from the amorphous phase. However, in these alloys the observation of only bcc phase forming initially from amorphous alloys with Co:Fe ratios well within the single phase fcc region of the binary phase diagram makes such an explanation unlikely. A discussion of the possibility of compositional partitioning resulting in bcc crystalline phase enriched in Fe can be found in Ref. 6 and seems to be quite likely in these alloys. It is well known that Co has been observed to partition to the amorphous phase in HiTPerm alloys,[9] and it is reasonable to assert that the tendency for bcc phase to form may be related to enrichment of the first crystalline phase to form in Fe. A third possibility for the observed tendency of bcc phase to form at low temperatures could be associated with the presence of very fine bcc crystalline grains in the as-cast amorphous alloys too small and disperse to be detected through XRD techniques. A possible observation of such fine bcc grains in an as-cast ribbon was noted in Ref. 6, and the growth of preexisting bcc crystallites could potentially explain the observations here and in previous studies.[5,6] The lack of detailed understanding of the structural and thermodynamic properties of the amorphous phase make a quantitative analysis of the thermodynamic factors governing the transformations of interest difficult at this time.

CONCLUSIONS

Crystallization of the Co-rich HiTPerm alloys invove interesting fundamental issues associated with the tendency for a bcc nanocrystalline phase to form more readily than fcc phase from the amorphous phase upon primary crystallization as compared to the predictions of the binary equilibrium phase diagram. Here it has been shown that with increasing Co:Fe ratio in HiTPerm alloys, fcc phase begins to form at lower temperatures and is observed in larger amounts for a given annealing temperature and time.

ACKNOWLEDGMENTS

The authors thank Vladimir Keylin and Spang Magnetics for assistance with field annealing processing of toroidal cores. Francis Johnson of General Electric is acknowledged for advice on electrical loss measurements and Matthew Willard of the Naval Research Laboratories is acknowledged for useful discussions and assistance with loss measurements. P.R.O. gratefully acknowledges funding through a National Defense Science and Engineering Graduate Research Fellowship (NDSEG). This work was funded by NSF Grant No. DMR-0406220. This work was also supported in part by the Army Research Laboratory and was accomplished under Cooperative Agreement No. W911NF-04-2-0017.

[1] M. E. McHenry *et al.*, Prog. Mater. Sci. **44**, 291 (1999).
[2] Y. Yoshizawa *et al.*, J. Appl. Phys. **64**, 6044 (1988).
[3] K. Suzuki, A. Makino, N. Kataika, A. Inoue, and T. Masumoto, Mater. Trans., JIM **32**, 93 (1991).
[4] M. A. Willard, M.-Q. Huang, D. E. Laughlin, M. E. McHenry, J. O. Cross, V. G. Harris, and C. Franchetti, J. Appl. Phys. **85**, 4421 (1999).
[5] Y. Yoshizawa, S. Fujii, D. H. Ping, M. Ohnuma, and K. Hono, Scr. Mater. **48**, 863 (2003).
[6] M. A. Willard, T. M. Heil, and R. Goswami, Metall. Mater. Trans. A (in press).
[7] I. Ohnuma, H. Enoki, O. Ikeda, R. Kainuma, H. Ohtani, B. Sundman, and K. Ishida, Acta Mater. **50**, 379 (2002).
[8] T. B. Massalski, *Relationships Between Metallic Glass Formation Diagrams and Phase Diagrams*, Proceeding of the Fourth International Conference on Rapidly Quenched Metals (The Japan Institute of Metals, Sendai, 1981), pp. 203–208.
[9] D. H. Ping, Y. Q. Wu, K. Hono, M. A. Willard, M. E. McHenry, and D. E. Laughlin, Scr. Mater. **45**, 781 (2001).
[10] M. A. Willard, T. Francavilla, R. Goswami, and V. G. Harris, Mater. Res. Soc. Symp. Proc. **851**, N.N.5.2.1 (2005).